Laser-assisted scattering from a one-dimensional δ-function potential: An exact solution

K. J. LaGattuta
Applied Theoretical Physics Division, Los Alamos National Laboratory, Los Alamos, New Mexico 87545
(Received 23 August 1993)

We consider the laser-assisted scattering of an electron by an attractive one-dimensional δ-function potential, and solve analytically a coupled-channel Lippmann-Schwinger equation for the full scattering amplitude. Energy, in multiples of the laser frequency, can be absorbed or emitted by the electron during the scattering, and the corresponding superelastic and inelastic, as well as the elastic, scattering amplitudes are all determined exactly. Stimulated recombination resonances are observed in all channels, if the laser irradiance is not too high ($I_0 \leq 10^{16}$ W/cm^2, for a binding energy of 0.5 a.u.) The resonance widths are a direct measure of the multiphoton ionization rates from the bound level. For stronger fields the resonances broaden and disappear into the background. For ultrastrong fields ($I_0 > 10^{17}$ W/cm^2) narrow structures reemerge just below multiphoton thresholds. An analytic continuation of the scattering amplitude into the complex energy plane is performed, and the poles of the scattering amplitude are located as a function of laser frequency and irradiance. The question of stabilization for this potential is reconsidered in the light of the present information.

PACS number(s): 34.80.Qb, 34.50.Rk, 32.80.Wr, 42.50.Hz

I. INTRODUCTION

A body of work now exists which describes the interaction of an electron with a laser electric field, while moving under the influence of an attractive δ-function potential in one dimension (1D). These approaches have involved, in some form, a numerical solution of the time-dependent Schrodinger equation [1–3]. Photoionization rates have been deduced for a range of laser parameters, throughout the strong-field regime (10^{13} W/cm^2 $\leq I_0 \leq 10^{16}$ W/cm^2), although not in the ultrastrong-field domain ($I_0 > 10^{16}$ W/cm^2). Scattering rates modified by the laser have not been considered for this potential. However, laser-assisted scattering has been discussed in several other contexts [4–10].

A possibility of the stabilization of bound states against photoionization, at high values of laser irradiance, has also been considered recently by many workers [11–16], for a variety of potentials. Although stabilization has generally been expected to appear at high irradiance and high frequency, the absence of stabilization was predicted for an electron moving in an attractive 3D δ-function potential, with a circularly polarized laser field [16]. Finally, an electron moving under the influence of a 1D δ-function potential, with a linearly polarized laser field, has been predicted to show both stabilization [17] and the absence of stabilization [18].

In the present work, we describe an exact solution of the laser-assisted scattering problem for an electron interacting with an attractive 1D δ potential. The coupled-channel Lippmann-Schwinger equation for the scattering amplitude $T^{(n_f,n_i)}(k_f,k_i;E)$ is solved in terms of a sum over analytic functions, where the number of photons in the laser field is n_i initially, and n_f finally, and we assume that both $n_i \gg 1$ and $n_f \gg 1$, so that the laser field can be treated classically. The scattering rate, as a function of the electron initial kinetic energy E_i, is obtained as

$$R_n(E_i)=(1/|k_f|)\left|\sum_{n_i} T^{(n_f,n_i)}(k_f,k_i;E)\right|^2 , \quad (1)$$

where the on-shell limit is such that $E_i=k_i^2/2$, $E_f=k_f^2/2$, $E=E_i+n_i\omega_0=E_f+n_f\omega_0$, and $n=n_f-n_i$ is the number of photons emitted during the scattering. If $n<0$, then net absorption occurs; $n=0$ corresponds to elastic scattering. We adopt the convention that the initial electron momentum k_i is positive, so that $k_f>0$ represents forward scattering, while $k_f<0$ denotes backward scattering. Atomic units (a.u.) are used throughout. Our formalism is similar to that of Faisal [4], who described scattering from a three-dimensional single-term separable potential, in the field of a circularly polarized laser.

The scattering rate [Eq. (1)] is evaluated for a range of laser parameters. Stimulated recombination resonances are observed, in all channels, if the laser irradiance is not too high, $I_0 < 10^{16}$ W/cm^2, for an underlying bound-state energy of -0.5 a.u. At higher irradiances these resonances broaden and disappear into the background. For ultrastrong fields ($I_0 > 10^{17}$ W/cm^2) sharp structures reappear just below multiphoton thresholds.

An analytic continuation of the scattering amplitude is performed, and the poles of the scattering amplitude are located as a function of complex energy, for a broad range of laser frequency and irradiance. An analysis of these results allows us to comment anew on the stabilization hypothesis for this system [17,18].

II. FORMALISM

We write the (time-dependent) Hamiltonian for this problem as

$$H=H_0-i(\partial/\partial x)(F_0/\omega_0)\cos(\omega_0 t) , \quad (2)$$

where the Hamiltonian in the absence of the laser field is

$$H_0 = -(\tfrac{1}{2})\partial^2/\partial x^2 - \delta(x) \ . \tag{3}$$

A bound state of H_0 exists at energy $E_B = -0.5$ a.u., with eigenfunction $\phi_B(x) = \exp(-|x|)$. The continua have energies $E > 0$, with (scattering) wave functions $\phi_k^{(+)}(x) = \exp(ikx) + (i/k)\exp(ik|x|)/(1 - i/k)$, and $k = \sqrt{2E}$. The corresponding on-shell scattering amplitude is $T(k',k;E) = -1/(1-i/k)$, for scattering from k to k', and where $k' = \pm k = \sqrt{2E}$. The scattering rate is then $R(E) = (1/|k'|)/(1+1/2E)$, independent of the sign of k'; see Fig. 1. A term $(\frac{1}{2})(F_0/\omega_0)^2\cos^2(\omega_0 t)$ has been deliberately omitted from Eq. (2), since it has no physical consequences [3,7] (in the dipole approximation).

In the strong-field regime the Hamiltonian might better be written as

$$H = H_{\rm em} - \delta(x) \ , \tag{4}$$

where the "electromagnetic Hamiltonian" is

$$H_{\rm em} = -(\tfrac{1}{2})\partial^2/\partial x^2 - i(\partial/\partial x)(F_0/\omega_0)\cos(\omega_0 t) \ . \tag{5}$$

The solutions of the time-dependent Schrödinger equation for $H_{\rm em}$ may be given as

$$\Psi_k(x,t) = \exp\{-ik^2 t/2 + ik[x - x_0\sin(\omega_0 t)]\} \ , \tag{6}$$

where $x_0 = F_0/\omega_0^2$ is the amplitude of the classical quiver motion. For fixed total energy E, these states can be Fourier transformed to yield

$$\Phi_k(x,E) = \sum_N \phi_k^{(N)}(x)\delta(E - k^2/2 - N\omega_0) \ , \tag{7}$$

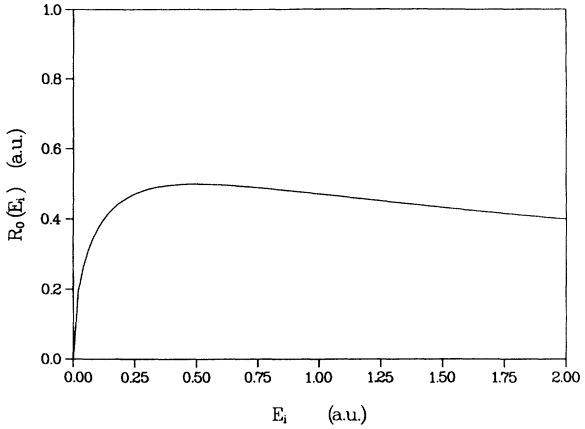

FIG. 1. The scattering rate vs E_i, for $x_0 = 0$; see discussion following Eq. (3).

where

$$\phi_k^{(N)}(x) = \exp(ikx)J_N(kx_0) \tag{8}$$

and J_N is the ordinary Bessel function of order N.

We choose the wave functions $\phi_k^{(N)}(x)$ as the asymptotic states, and write the Lippmann-Schwinger equation for scattering by the δ-function potential, in the field of the laser, as

$$T^{(N',N)}(k',k;E) = V^{(N',N)}(k',k) + \sum_{N''}\sum_{N'''}\int (dk''/2\pi)V^{(N',N'')}(k',k'') \times \int (dk'''/2\pi)\int dE' G^{(+)}_{N'',N'''}(k'',k''';E,E')T^{(N''',N)}(k''',k;E') \tag{9}$$

where the matrix elements of the scattering potential $V(x) = -\delta(x)$ are

$$V^{(N',N)}(k',k) = -J_{N'}(k'x_0)J_N(kx_0) \ . \tag{10}$$

The Green's function in the field (but without the scattering potential) is given by

$$G^{(+)}_{N',N}(k',k;E',E) = 2\pi J_{N'}(k'x_0)J_N(kx_0)\delta(k'-k)\delta(E'-E-[N'-N]\omega_0)/(E - N\omega_0 - k^2/2 + i\eta) \ , \tag{11}$$

where η is a positive infinitesimal.

We have obtained the solution of Eq. [9] exactly as

$$T^{(N',N)}(k',k;E) = -J_{N'}(k'x_0)J_N(kx_0)/[1+\chi(E)] \ , \tag{12}$$

where $\chi(E)$ is defined by

$$\chi(E) = \sum_N \int (dk/2\pi)J_N^2(kx_0)/(E - N\omega_0 - k^2/2 + i\eta) \ . \tag{13}$$

In the preceding, all sums and integrals extend from $-\infty$ to $+\infty$. Finally, the scattering rate was obtained from Eqs. (1) and (13) as

$$R_n(E_i) = (1/|k_f|)\left|\sum_{n_i} J_{n_i+n}(k_f x_0)J_{n_i}(k_i x_0)\Big/[1+\chi(E_i+n_i\omega_0)]\right|^2 \ . \tag{14}$$

Note that, in Eq. (14), the sum over n_i involves the argument of χ as well as the order of the Bessel functions. Consequently, the performance of this sum is a nontrivial exercise, generally requiring the applications of a high-speed computer.

At first sight, a further complication resides in the fact that the evaluation of the individual integrals in Eq. (13) cannot in general be performed analytically. However, we have shown that, when the (N-dependent) principal value components are summed over their full range, the result is precisely zero. Consequently, one has for real E that

$$\chi(E)=-i\sum_N J_N^2[\sqrt{2(E-N\omega_0)}x_0]/\sqrt{2(E-N\omega_0)}\ , \tag{15}$$

which is an exact result. Now with the aid of Eq. (15), the scattering rates given by Eq. (14) can be explicitly computed as a function of the incoming energy E_i. Although the sums in Eqs. (14) and (15) extend formally from $-\infty$ to $+\infty$, upon evaluation convergence is obtained with a finite number of terms. The necessary number of terms depends on the values of I_0 and ω_0, and on the desired accuracy. In generating our results (see Sec. III) less than 100 terms were required, provided that the "convergence parameter" $F_0^2/4\omega_0^3<6$. For larger values of this parameter, accuracy deteriorates even in double precision, due to the appearance in Eq. (15) of exponentially large terms with alternating sign. An efficient algorithm was employed to compute the Bessel functions, the argument of which is either purely real ($E\geq n\omega_0$) or purely imaginary ($E<n\omega_0$); i.e., for Im $E=0$.

It may be worth pointing out that the laser field in Eqs. (2) and (5) can really only be defined up to a phase so that, in fact, $\cos(\omega_0 t)$ should be replaced by $\cos(\omega_0 t+\phi)$, and ϕ carried through to the end of the calculation. Finally, R_n should be averaged over ϕ. However, the entire effect of this arbitrary phase on the scattering amplitude is contained in an n-dependent multiplicative factor of modulus 1; i.e., $T^{(n_i+n,n_i)}\rightarrow T^{(n_i+n,n_i)}\exp(in\phi)$. This does not affect the scattering rate R_n. Arguing again on an intuitive basis, one expects R_n to be insensitive to the laser phase if the spatial extent of the incoming wave packet is much greater than the amplitude of the quiver motion x_0. The modulated plane waves [Eq. (8)] employed here extend over all space, so that this criterion is certainly satisfied. Moreover, wave packets can be constructed from the functions appearing in Eq. (8) which will easily satisfy this condition.

III. RESULTS

The scattering rate for zero external field ($x_0=0$) appears in Fig. 1. It shows no sharp features, and forward and backward scattering rates are identical.

In Fig. 2, we display the elastic scattering rate for $\omega_0=1.0$ a.u. and $x_0=0.25$ a.u. (corresponding to $I_0=2.2\times10^{15}$ W/cm^2). Resonance structures appear at $E_i\approx n\omega_0-0.5$ a.u., where $n=1$ and 2. These are "stimulated recombination" resonances. (We prefer this nomenclature to the sometimes used "capture-escape" resonance. Since every scattering resonance follows a path of first capture, then escape, this latter term seems to us to be insufficiently descriptive.) The forward (solid line) and backward (dashed line) scattering rates are now different. Generally, backward elastic scattering is suppressed in the field of the laser. We will return to this point below.

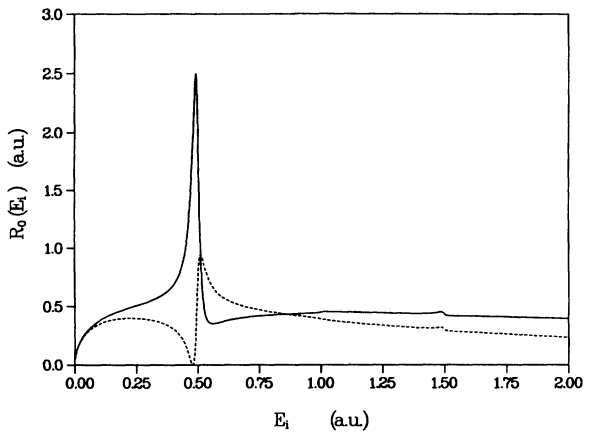

FIG. 2. The elastic scattering rate vs E_i, for $\omega_0=1.0$ a.u. and $x_0=0.25$ a.u.; forward scattering (solid line); and backward scattering (dashed line).

It seems useful to point out here that the scattering amplitude is periodic in the sense that, if a pole of T exists on the n_ith sheet at $E_i=A_i-iB_i$, with both A_i and B_i real and positive, then poles also exist on the same sheet at $E_i=A_i+m\omega_0-iB_i$, where m is an integer (positive or negative) or zero, provided that $A_i+m\omega_0\geq0$. These poles lead to a series of stimulated recombination resonances. The minimum value of m produces a peak at the lowest allowed value of the incoming electron energy. Larger values of m produce peaks at higher values of the electron energy, with recurrent peaks separated by ω_0. These resonances correspond, in photoionization, to threshold and above-threshold-ionization (ATI) peaks, respectively. The full widths ($\Gamma=-2B_i$) of the threshold and ATI peaks are formally identical. However, actual peak shapes may differ considerably due to interference with the energy-dependent background term.

We now consider the structure of an individual resonance in more detail. The expected position of the lowest-lying resonance in Fig. 2 is at $E_i=\omega_0-0.5-\Delta_1=0.496$ a.u., where the shift to lowest order in x_0 is $\Delta_1=(x_0^2/4)(2-\sqrt{2\omega_0})=0.067$ a.u., and the full width to lowest order is $\Gamma_1=(x_0^2/2)\sqrt{2\omega_0-1}=0.031$ a.u.; see Appendix. These predicted values agree well with the measured values taken from Fig. 2. The Keldysh parameter ($\gamma=1/x_0\omega_0$) is $\gamma=4.0$, well inside the photoabsorption domain.

The occurrence of a resonance peak for forward scattering, and a corresponding minimum for backward scattering, can easily be understood. Let the elastic-scattering amplitude be approximated by

$$T(k',k;E_i)\approx -1/(1-i/k)+\langle k'|-i(\partial/\partial x)(F_0/2\omega_0)|B\rangle\langle B|-i(\partial/\partial x)(F_0/2\omega_0)|k\rangle/(E_i-E_B-U_p-\omega_0+i\Gamma_1/2) \tag{16}$$

for $E_i=k^2/2=k'^2/2$, where in the coordinate representation $\langle x|k\rangle=\phi_k^{(+)}(x)$ and $\langle x|B\rangle=\phi_B(x)$ (see Sec. II), and where Γ_1 is the width of the ground state. The matrix elements in Eq. (16) can be evaluated explicitly, yielding

$$T(k'k;E_i)\approx -1/(1-i/k)+(F_0/\omega_0)^2[kk'/(1+k^2)^2]/(k^2/2-0.5-U_p-\omega_0+i\Gamma_1/2)\ . \tag{17}$$

In the neighborhood of the resonance, the terms due to scattering from the δ-function potential (first term on the right-hand side), and to stimulated recombination followed by photoionization (second term), interfere either constructively or destructively, depending upon the sign of k', as can be verified from Eq. (17) explicitly.

In Fig. 3, we also consider a higher irradiance $I_0=3.5\times10^{16}$ W/cm^2 for $\omega_0=1.0$ a.u. ($\gamma=1.0$). The resonances are now very broad. The lowest-lying resonance appears at a position $E_i=0.395$ a.u., with a measured width $\Gamma_1=0.41$ a.u. At this high irradiance, the lowest-order calculation does rather poorly, predicting values of $E_i\approx\omega_0-0.5-\Delta_1=0.43$ a.u., and $\Gamma_1=0.55$ a.u. Note the appearance of sharp cusps at multiphoton thresholds [19]; i.e., at $E_i=n\omega_0$, for $n=1$ and 2.

Extending the calculation again to higher irradiances, for $I_0=1.4\times10^{17}$ W/cm^2 and $\omega_0=1.0$ a.u. ($\gamma=0.50$), we obtain the results appearing in Fig. 4. The resonance structure is now attenuated, partly as an effect of an increase in the amount of background scattering. However, the resonance peaks also seem to be narrowing. At still higher irradiances the resonance disappears almost entirely into the background, and a very sharp cusp appears; see Fig. 5(a). As the irradiance increases still further, the cusp inverts and a sharp resonancelike structure emerges just below the cusp; see Figs. 5(b) and 5(c).

This initial disappearance of resonances at very high irradiance, which we have also observed over a range of laser frequencies, seems to be in accordance with the prediction that stabilization would not occur for a 1D δ-function potential [18]. However, as has just been demonstrated, a close inspection of the scattering rate in the vicinity of the multiphoton threshold does show the reemergence, at large x_0, of a sharp resonancelike structure just below the cusp; see Fig. 6. This seems to be a general phenomenon.

In order to consider the question of resonance behavior more closely, we investigated the pole structure of the scattering amplitude. From Eq. (14), zeros of $1+\chi(E_i+n_i\omega_0)$, as a function of complex E_i, were located on a family of sheets, for which $-n_i=1,2,3,\ldots$. These zeros correspond to poles of the scattering amplitude at values $E_i\equiv E_{\rm res}=\mathrm{Re}E_{\rm res}+\mathrm{Im}E_{\rm res}$, where $-\mathrm{Im}E_{\rm res}=\Gamma_{-ni}/2$, and Γ_{-ni} is the photoionization rate, on the n_ith sheet. In accordance with the discussion of Ref. [20], we insure that the poles which we uncover are "physical," and not "shadow" poles. That is, we insure that both Re $k_{ni}>0$, for *all* open channels, and Im $k_{ni}>0$, for *all* closed channels, simultaneously. The channel momenta are given by $k_{ni}=\sqrt{2(E_i+n_i\omega_0)}$. An open channel is such that $\mathrm{Re}(E_i+n_i\omega_0)\geq 0$, and a closed channel satisfies $\mathrm{Re}(E_i+n_i\omega_0)<0$.

For example, in Fig. 7 we plot values of the half width $-\mathrm{Im}E_{\rm res}$ vs x_0 for $\omega_0=0.4$ a.u. If $x_0\ll 2.0$ a.u., then the half width rises as $(4\omega_0-1)^{3/2}x_0^4/64$, as expected for this initially two-photon process; see Appendix. For values of $x_0\geq 2.0$ a.u., the width decreases, and then abruptly "vanishes"; i.e., the pole disappears on the $-n_i=2$ sheet. There is a small gap in x_0 values, centered around $x_0=2.4$ a.u., where no pole exists anywhere in the multisheeted complex E_i space. Then for x_0 slightly greater than 2.4 a.u., a pole appears on the $-n_i=3$ sheet. This sequence of migrations of the resonance pole to higher sheets continues as x_0 increases. For x_0 large enough, poles on several different sheets may coexist, for

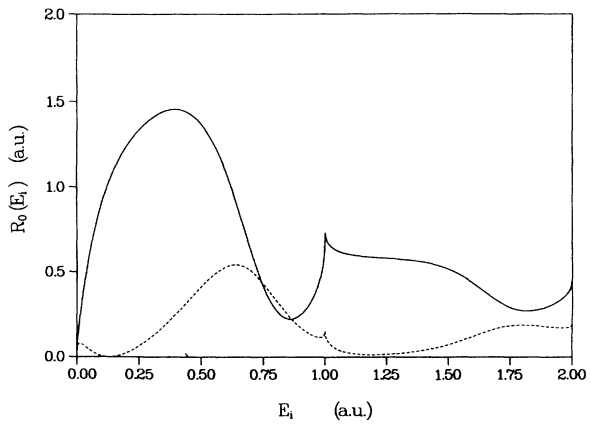

FIG. 3. Same as Fig. 2, but for $x_0=1.0$ a.u.

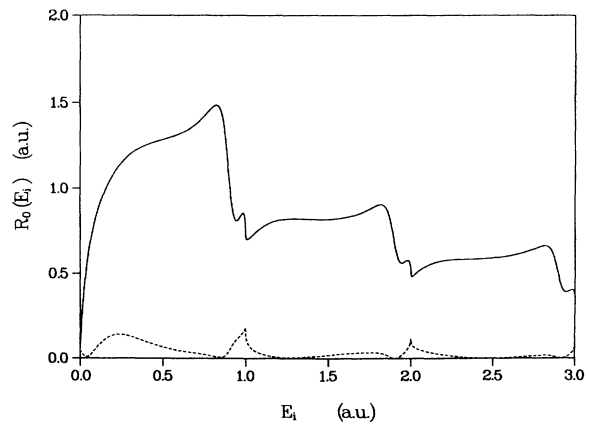

FIG. 4. Same as Fig. 2, but for $x_0=2.0$ a.u.

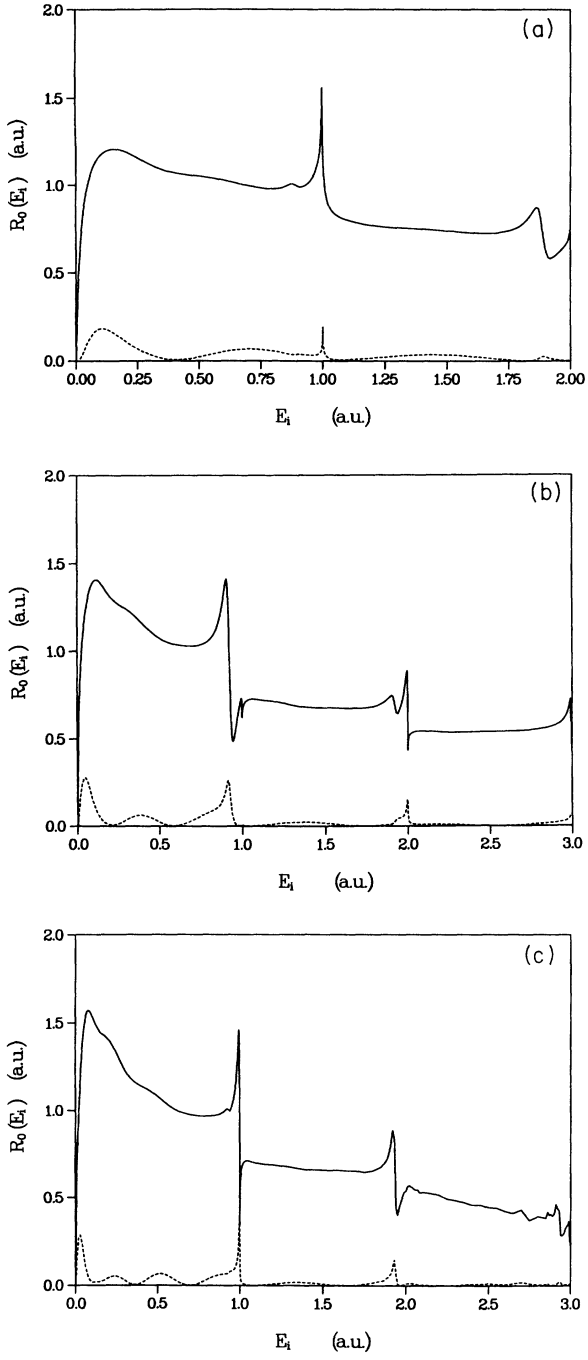

FIG. 5. (a) Same as Fig. 2, but for $x_0=3.0$ a.u. (b) Same as Fig. 2, but for $x_0=4.0$ a.u. (c) Same as Fig. 2, but for $x_0=5.0$ a.u.

$\omega_0=0.4$ a.u. In the language of Ref. [20], poles which correspond to unphysical or shadow states, at small values of x_0, may emerge on the physical sheet at larger values of x_0.

In Fig. 8 we plot values of $-\mathrm{Im}E_{\mathrm{res}}$ vs x_0 for $\omega_0=0.8$ a.u. As expected, for this initially one-photon process the half width rises as $(2\omega_0-1)^{1/2}x_0^2/4$, for $x_0 \ll 1$; see Appendix. However, this pole does not disappear at large x_0, but persists along with other poles on sheets for which $-n_i > 2$. There is no indication of the disappearance of poles at the highest x_0 values, except for $-n_i=2$. Consequently, one might expect that stabilization can be achieved for this case, if the smallest width dominates the photoionization rate. For example, for $x_0=5.0$ a.u., the most long-lived state lives on the $-n_i=1$ sheet, and has a half width 0.022 a.u., which falls with increasing x_0 as $1/x_0^2$.

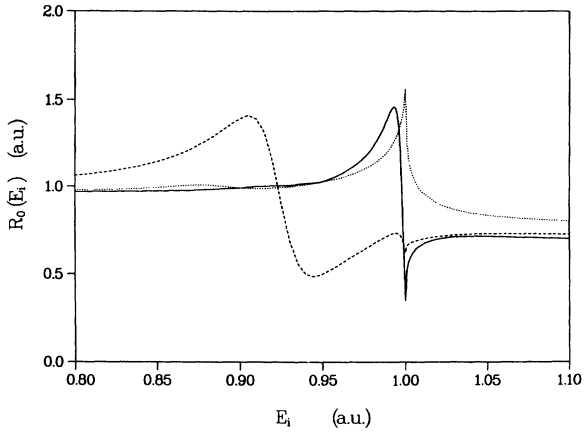

FIG. 6. Detail of Fig. 5, for $x_0=3.0$ (dotted curve), 4.0 (dashed curve), and 5.0 (solid curve) a.u.

It is also instructive to consider the real part of the resonance energy. In Fig. 9, we plot $\mathrm{Re}E_{\mathrm{res}}+n_i\omega_0$ for $\omega_0=0.4$ a.u. This quantity corresponds to the effective binding energy, on the n_ith sheet. It is clear, in this case, that the binding energy decreases (the electron becomes more deeply bound) as the laser irradiance increases. However, "transitions" between successive branches of the resonance trajectory must also occur, if this state is to evolve quasicontinuously; see Fig. 7 for a plot of the corresponding imaginary part.

In Fig. 10, we plot $\mathrm{Re}E_{\mathrm{res}}+n_i\omega_0$ for $\omega_0=0.8$ a.u. Now there is a loosely bound state at large x_0 which is continuously connected to the bound state at $x_0=0$; the imaginary part, for this case, appears in Fig. 8.

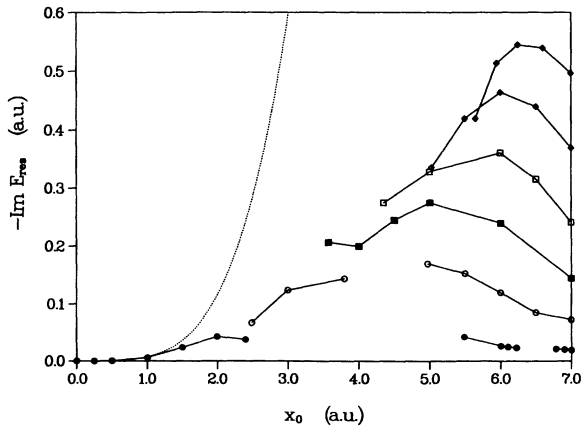

FIG. 7. Values of $-\mathrm{Im}E_{\mathrm{res}}$ are plotted vs x_0, for $\omega_0=0.4$ a.u. Successive branches of the resonance trajectory appear on the physical sheet as x_0 increases. The prediction of the lowest-order calculation is shown by the dotted line.

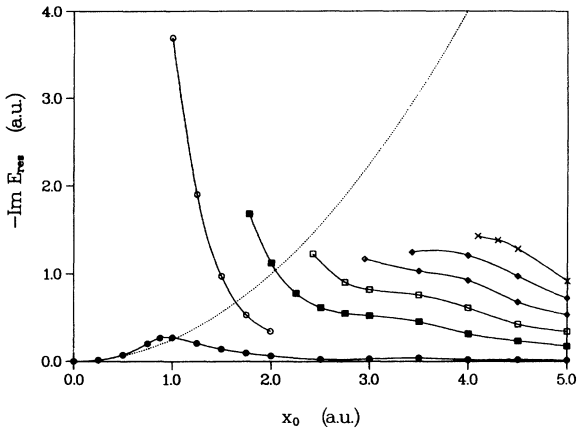

FIG. 8. Same as Fig. 7, but for $\omega_0=0.8$ a.u.

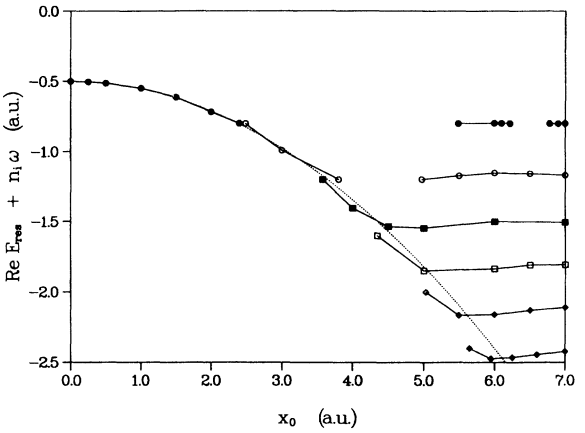

FIG. 9. Values of $\mathrm{Re}E_{\mathrm{res}}+n_i\omega_0$ are plotted for $\omega_0=0.4$ a.u. Successive branches of the resonance trajectory appear on the physical sheet as x_0 increases. The prediction of the lowest-order calculation is shown by the dotted line.

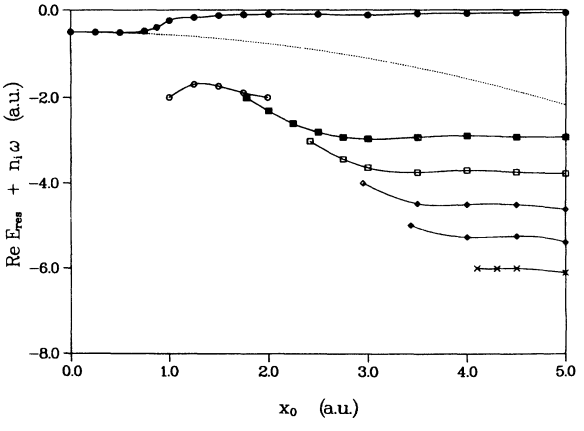

FIG. 10. Same as Fig. 9, but for $\omega_0=0.8$ a.u.

From these observations we can say that an adiabatic increase in the irradiance from small to large values will leave the electron in the state with the narrowest width, if this state connects continuously with the zero irradiance bound state; e.g., when $\omega_0 \gg 0.5$ a.u. In this case, stabilization is likely. However, if the connection is discontinuous, then there must be a transition between the quasi-bound states, as the irradiance increases. In this case, stabilization is unlikely to occur.

IV. SUMMARY

We have considered the scattering of an electron by an attractive 1D δ-function potential, while moving in a sinusoidally varying electric field. The Lippmann-Schwinger equation for the coupled-channel scattering amplitude was solved exactly.

Explicit calculation of the scattering rate, for a range of frequencies and field strengths, revealed the presence of stimulated recombination resonances. At fixed frequency, as the field strength was increased from small values, these resonances first broadened, but then narrowed again, for $F_0^2/4\omega_0^3 > 5$ a.u. The appearance of cusps at multiphoton thresholds tended to mask this resonance narrowing.

A calculation of the trajectory of the poles of the coupled-channel scattering amplitude in the complex energy plane suggested an adiabatic stabilization of the underlying bound state, provided that the frequency was high enough. At low frequency, adiabatic stabilization was absent, due to discontinuities in the resonance trajectory. In this context, it is interesting to note that the emergence of shadow states on the physical sheet, at high-field strength, is a general phenomenon for this system, and several such states can exist simultaneously. Conversely, there are regions of relatively low frequency and relatively high-field strength for which no physical state exists. Similar phenomena have been reported previously for other systems [20].

We emphasize that our explicit results are confined to a range of frequencies $0.1 \leq \omega_0 \leq 2.0$ a.u., and to a range of field strengths such that $F_0^2/4\omega_0^3 < 6$ a.u. Consequently, we are not yet able to comment on conjectures relating to the behavior of the width at asymptotically high frequency [17], nor at asymptotically large x_0.

For example, it is consistent with our results to speculate that just one physical state will persist as $x_0 \to \infty$, at high frequency, and that this state evolves continuously from the state existing at $x_0 \to 0$. In this case, adiabatic stabilization would exist, in the high-frequency limit. However, it may also be that the trajectory evolving from the state existing at $x_0 \to 0$ becomes discontinuous, within some range of very large-x_0 values, even at high frequency. In this case, adiabatic stabilization would not exist. Still more work in this area is required in order to resolve this issue.

APPENDIX

Resonances appear at zeros of the denominators in Eq. (14), on the physical sheet [20] in the complex energy (E_i) plane. These zeros can be located easily, as $x_0 \to 0$, espe-

cially for low photon order.

For example, for a one-photon process, a resonance occurs at a value of the complex energy E_i such that

$$0=1+\chi(E_i-\omega_0) . \tag{A1}$$

Using Eq. (13), and expanding χ in powers of x_0, we obtain

$$0\simeq 1-i\{1/\sqrt{2(E_i-\omega_0)} -[x_0^2/4)(2\sqrt{2(E_i-\omega_0)} -\sqrt{2E_i}-\sqrt{2(E_i-2\omega_0)}]+\text{h.o.t.}\} , \tag{A2}$$

where h.o.t. denotes terms of order x_0^4 and higher. Then, defining the energy as

$$E_i=\omega_0-0.5-\delta/2 , \tag{A3}$$

and expanding the right-hand side of Eq. (A2) in powers of δ, we obtain

$$\delta\simeq(x_0^2/2)[(2-\sqrt{2\omega_0+1})+i\sqrt{2\omega_0-1}]+\text{h.o.t.} \tag{A4}$$

The shift in the underlying bound-state energy is, therefore,

$$\Delta_1\simeq(x_0^2/4)(2-\sqrt{2\omega_0+1})+\text{h.o.t.} \tag{A5}$$

while the full width of the resonance state is

$$\Gamma_1\simeq(x_0^2/2)\sqrt{2\omega_0-1}+\text{h.o.t.} \tag{A6}$$

Notice that the shift Δ_1 is not generally equal to the ponderomotive energy, and can even have the opposite sign (at high frequency); i.e.,

$$\Delta_1\simeq(x_0^2/4)(2-\sqrt{2\omega_0+1})\neq(x_0\omega_0/2)^2 . \tag{A7}$$

For a two-photon process, a similar analysis shows that

$$\Delta_2\simeq(x_0^2/4)(2-\sqrt{2\omega_0+1}-\sqrt{1-2\omega_0})+\text{h.o.t.} \tag{A8}$$

and

$$\Gamma_2\simeq(4\omega_0-1)^{3/2}x_0^4/32+\text{h.o.t.} \tag{A9}$$

In this case, the shift reduces to the ponderomotive energy in the small-ω_0 limit.

These results can be generalized to arbitrarily high photon order (for lowest nonvanishing order in x_0. For example, for a n_i-photon process, the full width is

$$\Gamma_{-ni}\simeq 2(-2n_i\omega_0-1)^{(-2n_i-1)/2} \times(x_0/2)^{-2n_i}/[(-n_i)!]^2+\text{h.o.t.} \tag{A10}$$

The preceding analysis pertains only if the "threshold factor" is large, i.e., $(-2n_i\omega_0-1)\gg\Gamma_{-n_i}$. For fixed x_0, as $(-2n_i\omega_0-1)\to 0$, then a more careful analysis is required. In this limit, for instance, one has that

$$\Gamma_1\simeq x_0^4/8+\text{h.o.t.} , \tag{A11}$$

so that the one-photon ionization rate is discontinuous at $\omega_0=\frac{1}{2}+\Delta_1$.

[1] S. Geltman, J. Phys. B **10**, 831 (1977).
[2] S. Susskind and R. Jensen, Phys. Rev. A **38**, 711 (1988).
[3] K. LaGattuta, Phys. Rev. A **40**, 683 (1989).
[4] F. Faisal, *Theory of Multiphoton Processes* (Plenum, New York, 1987).
[5] I. Berson, J. Phys. B **8**, 3078 (1975).
[6] M. Mittleman, *Theory of Laser-Atom Interactions* (Plenum, New York, 1982).
[7] P. Milonni and J. Ackerhalt, Phys. Rev. A **39**, 1139 (1989).
[8] R. Sacks and A. Szoke, Phys. Rev. A **40**, 5614 (1989).
[9] S. Varro and F. Ehlotzky, J. Opt. Soc. Am. B **7**, 537 (1990).
[10] L. Collins and G. Csanak, Phys. Rev. A **44**, R5343 (1991).
[11] J. Gersten and M. Mittleman, J. Phys. B **9**, 2561 (1990).
[12] M. Pont and M. Gavrila, Phys. Rev. Lett. **65**, 2362 (1990).
[13] M. Dorr, R. Potvliege, and R. Shakeshaft, Phys. Rev. Lett. **64**, 2003 (1990).
[14] H. Reiss, Phys. Rev. A **46**, 391 (1992).
[15] M. Fedorov, M. Ivanov, and A. Movsesian, J. Phys. B **23**, 2245 (1990).
[16] V. Krainov and M. Preobrazhenskii, Zh. Eksp. Teor. Fiz. **103**, 1143 (1993) [Sov. Phys. JETP **76**, 559 (1993)]; F. Faisal, P. Filipowicz, and K. Rzazewski, Phys. Rev. A **41**, 6176 (1990).
[17] T. Grozdanov and P. Krstic, Phys. Lett. A **149**, 144 (1990).
[18] S. Geltman, Phys. Rev. A **45**, 5293 (1992).
[19] F. Faisal and P. Scanzano, Phys. Rev. Lett. **68**, 2909 (1992).
[20] R. Potvliege and R. Shakeshaft, in *Atoms in Intense Laser Fields*, edited by M. Gavrila (Academic, New York, 1993).